Research Article

In Silico Evaluation of Biopharmaceutical Properties of Chloramphenicol Derivatives and their Iron Complexes

Kananda Masonga Michel, Lumbwe Kitenge Edouard, Kayembe Kazadi Oscar, Mbayo Kitambala Marsi, Kalonda Mutombo Emery*

Department of Chemistry, Faculty of Science, University of Lubumbashi, DR Congo

***Corresponding author:** Kalonda Mutombo Emery, Department of Chemistry, University of Lubumbashi, Lubumbashi, Democratic Republic of Congo

Received: 17 October 2021; **Accepted:** 16 November 2021; **Published:** 04 March 2022

Citation: Kananda Masonga Michel, Lumbwe Kitenge Edouard, Kayembe Kazadi Oscar, Mbayo Kitambala Marsi, Kalonda Mutombo Emery. *In silico* Evaluation of Biopharmaceutical Properties of Chloramphenicol Derivatives and their Iron Complexes. Journal of Bioinformatics and Systems Biology 5 (2022): 44-57.

Abstract

Context and objectives

The use of chloramphenicol (CAM) has been reduced due to the side effects associated with its use (Bone marrow depression, neurotoxicity) and the increase in resistance to CAM that some microbes develop. To overcome these difficulties, two CAM derivatives, L1 and L2, and their respective iron complexes were synthesized to evaluate in silico their biopharmaceutical properties.

Methodology

Chloramphenicol, acetaminophen, and acetylsalicylic acid were purified from commercial pharmaceuticals. Synthesized compounds were characterized by staining tests and by UV-visible spectrophotometry. These were subjected to specialized bioinformatics tools such as PreADMET, and PkCSM, which allowed in silico prediction of ADMET properties and the Molinspiration tool was used to determine bioactivity scores of the synthesized products.

Results

The substrate (CAM), as well as the basic reagents (AAP and AASC) were purified from commercial pharmaceuticals. The CAM derivatives (L1 and L2) and also their iron complexes (C1, C2, and C3) were synthesized and showed maximum absorbance at 335 nm for CAM, 325 nm for L1, 395 nm for L2, at 330 nm for C1, at 325 nm for C2, and at 335 nm for C3. The in silico simulations performed with the above-mentioned tools showed that all the ligands (CAM, L1, and L2) present good similarities with the drugs, a good bioavailability because they were compliant with the Lipinski rule. The complexes, although bioavailable, did not conform to Lipinski's rule. CAM showed efficacy in enzymatic inhibition. However, L1 and L2 ligands perform better in ion channel modulation, kinase, and protease inhibition. This suggests that the ligands have better therapeutic performance and may well address several clinical needs. The C3 complex was the compound that showed better bioavailability and high bioactivity thus it was the most bioactive.

Conclusion

L1, L2, and C3 could therefore be potential and promising candidates for CAM substitution.

Keywords: Chloramphenicol; Complex; Bioavailability; Synthesis; Prediction; ADMET

Abbreviation

ADMET: Absorption, Distribution, Metabolism, Extrusion, and Toxicity; **MM** : Molecular Mechanics; **OPLS** : Optimized Potentials for Liquid Simulations; **AMBER** : Assisted Molecular Building and Energy Refining ; **EMO** : Energy Of Molecule; **UFF** : Universal Force Field ; **ADME** : Absorption, Distribution, Metabolism, Extrusion ; **CCP** : Cellular Permeability of Caco-2; **BBB** : Blood-Brain Barrier ; **HIA**: Human Intestinal Absorption ; **MDCK** : Madin-Darby canine kidney; P-gp : P-glycoprotein; **ATP** : Adenosine triphosphate; **PPB** : Plasma protein binding ; **SP** : Skin Permeability ; **hERG** : human Ether-a-go-go-Related Gene); **GPCR** : G protein-coupled receptor; **NRL** : Nuclear receptor ligand ; **ICM** : Ion channel modulation; **KI** : Kinase inhibition ; **PI** : Protease inhibition ; **EI**: Enzyme activity inhibition ; **MLCT**: Metal to Ligand Charge Transfer ; **AAP**: Acetaminophen ; **AASC**: Acetylsalicylic acid ; **CAM** : Chloramphenicol ; **C1** : Ferric complex of CAM-O-AAP (L1) ; **C2**: CAM-O-AASC iron complex (L2) ; **C3**: CAM iron complex ; **FeCAM** : CAM iron complex; **FeCAM-O-AAP** : CAM-O-AAP iron complex (L1) ; **FeCAM-O-AASC** : CAM-O-AASC iron complex (L2) ; **L1** : 2-(4-Acetylaminophenoxy)-2-chloro-N-[1,3-dihydroxy-1-(4-nitrophenyl) propan-2-yl] acetamide "CAM-O-AAP; **L2**: 2-(2-Acetoxybenzoyloxy)-2-chloro-N-[1,3-dihydroxy-1-(4-nitrophenyl) propan-2-yl] acetamide "CAM-O-AASC1.

1. Introduction

The CAM, a bacteriostatic antibiotic of the phenicol family, has an effective bacteriostatic action against gram-positive and gram-negative bacteria and was the first broad-spectrum antibiotic to be used medically against typhoid infections. Although effective, its use is nowadays reduced because of its side effects and the increase of resistance developed by microbes and bacteria [1,2]. The CAM was first isolated in 1947 from *Streptomyces venezuelae*, and

was introduced two years later in clinical trials. This antibiotic works by inhibiting protein synthesis by binding to the bacterial ribosome center peptidyl transferase [3]. Over the years, the CAM has proven to be an extremely useful antibiotic for the therapy of various types of infection. Originally known as an inhibitor of bacterial protein synthesis, in some cases it can also exhibit bactericidal activity, especially against the three most common causes of meningitis, *Haemophilus influenzae*, *Streptococcus pneumonia*, and *Neisseria meningitidis* [4]. The CAM is generally considered a standard antimicrobial in the treatment of typhoid fever almost everywhere in the world due to its low price, established efficacy, and availability in oral and parenteral formulations. It is commonly recommended for the treatment of central nervous system infections because it is a molecule that crosses the blood-brain barrier more effectively and has good activity against most central nervous system pathogens [5]. Its use has been reduced markedly nowadays due to the increase of resistance developed by microbes and bacteria and its side effects such as neurotoxicity, bone marrow depression, severe aplastic anemia. Resistance or decreased susceptibility to chloramphenicol is frequently mediated by several phenomena such as mutations in ribosomal binding site residues. To circumvent the adverse effects following the administration of chloramphenicol, the interest in CAM derivatives is based on the improvement of therapeutic efficacy and the decrease of microbial resistance to CAM. Generally speaking, most of the chloramphenicol derivatives have shown decrease in toxicity, however, with a more or less slight loss of pharmaceutical efficacy [6]. Thus, it is necessary and paramount to obtain derivatives with better therapeutic performance that can substitute chloramphenicol. Thus, this work aimed to synthesize and predict *in silico* the pharmaco-biological properties of CAM derivatives and their Iron (III) complexes. The first derivative L1 is the reaction product of chloramphenicol with acetaminophen (AAP) and the second L2 is obtained with acetylsalicylic acid (AASC). Both reactants are potent analgesics and show good biological properties. The predictions of pharmaco-biological properties were performed using tools namely PreADMET, PkCSM, and Molinspiration software which are powerful tools in the field of bioinformatics and cheminformatics.

2. Methodology

2.1 Raw materials

The substrate used, chloramphenicol, as well as the reagents, acetaminophen, and acetylsalicylic acid were obtained from commercial pharmaceuticals (Table 1). The purification process concentrated the active ingredient and separated it from the starch, microcrystalline cellulose and, talc that constitute the excipient package.

2.2 Apparatus and software

Product purity was assessed by TLC on silica gel plates eluted with Methanol/Ethyl Acetate (1:1) and developed with iodine. UV-Vis spectra were recorded using a HACH DR 6000 UV-Vis spectrophotometer in methanol.

Modeling for finding the minimum energy of the complex stabilization was done using the molecular mechanics method with the UFF basis as presented by Bouchareb, Feng, and Ghannay et al. [7,8]. In addition, predictions of ADMET properties were performed using the Pre-ADMET and PkCSM tools and determination of bioactivity scores were performed using the Molinspiration tool.

2.3 Extraction, purification, and identification of chemicals used

For CAM, open the capsules and collect the powder. Weigh an amount equivalent to 20 g of chloramphenicol (80 capsules) and dissolve them in 100 ml of ethyl acetate in a beaker. Heat while stirring the mixture until boiling to ensure total dissolution of the solutes; Filter while hot, then let the filtrate cool until crystals form; Filter and dry under vacuum, then collect the residue greenish-white (Yield: 80%). For its identification, add to 1 g of CAM, a mixture of 5 drops of phenol, and 0.20 g of potassium hydroxide. Bring to a boil over a small flame and shake; a red-brown coloration develops. A red-orange color is produced and ammonia is released when the CAM is heated with a 50% sodium hydroxide solution [9]. For PAA, weigh 20 g of PAA equivalent to 40 paracetamol tablets and dissolve in 100 ml of acetone in a beaker. Heat while stirring the mixture until boiling to ensure total dissolution of the solutes. Filter while hot and collect the filtrate. Evaporate the solvent by heating, then collect the white crystals (Yield: 70%). For its identification, dissolve 0.10 g of PAA in 10 ml of water and add 0.5 ml of ferric chloride 25g/l; it appears an intense blue coloration (European Pharmacopoeia, 2017). For AASC, weigh 25 g of AASC equivalent to about 50 aspirin tablets and dissolve in 60 ml of isopropanol in a beaker; Heat while stirring the mixture until boiling to ensure total dissolution of solutes; Filter while hot, and collect the filtrate; Allow the filtrate to cool, and add about 180 ml of ice-cold distilled water; Collect the precipitates by vacuum filtration (Blank, yield: 79%). Finally, TLC evaluated the purity. To identify it, heat 0.5 mg of AASC in a test tube; the molten product gives off a strong acetic acid smell. Further heating turns the product from yellow to brown to black. Place a small amount of the AASC on a white ceramic plate or watch glass placed on a white background and add 1 drop of potassium hydroxide in ethanol. After 1 minute, add 1 drop of ferric chloride 25 g/l; a purple coloration appears [10].

2.4 Synthesis and identification of ligands and complexes

The ligand syntheses were done as described by Omar et al. [11] and the complex syntheses as described by Lawal and Obaleyo [12]. The formation of the products proceeds from the formation of the ether function (R-O-R) between the carbocation of CAM and the hydroxyl function of PAA and/or AASC. The ether function can form the oxonium ion in an acidic medium. However, the C-O bond can be broken, in the presence of hydrogen halide [13]. This is the basis for the identification of the ether function.

2.4.1. Synthesis of the ligand CAM-O-AAP (L1): In a 100 ml flask equipped with a refrigerator and a magnetic bar is introduced a mixture of acetone (70 ml), CAM (10 g, 0.03 mol), APP (3.596 g, 0.0238 mol), and sodium carbonate (2.524 g, 0.0238 mol). The reaction mixture is heated at reflux. After 5 hours, it is hot filtered, then the filtrate is cooled and left for 48 hours for crystallization. The residue is filtered and the crystals obtained are washed with ethanol (Yellowish-white, yield: 91.17%).

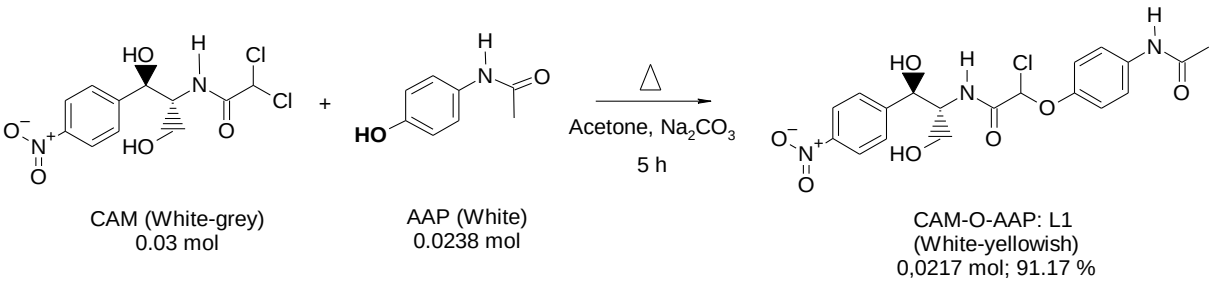

Figure 1: CAM-O-PAA synthesis equation

2.4.2. Synthesis of the ligand CAM-O-AASC (L2): In a flask (100 ml) equipped with a refrigerator and a magnetic bar is introduced a mixture of acetone (70 ml), CAM (10 g, 0.03 mol), AASC (4.2867 g, 0.0238 mol), and sodium carbonate (2.524 g, 0.0238 mol). The reaction mixture is heated at reflux. After 5 hours, it is filtered while hot. After cooling, two phases were observed, the non-ketone phase was washed with acetone, dried with Na2SO4, collected (Brown liquid, yield: 81%) and finally the purity of the product was evaluated by TLC.

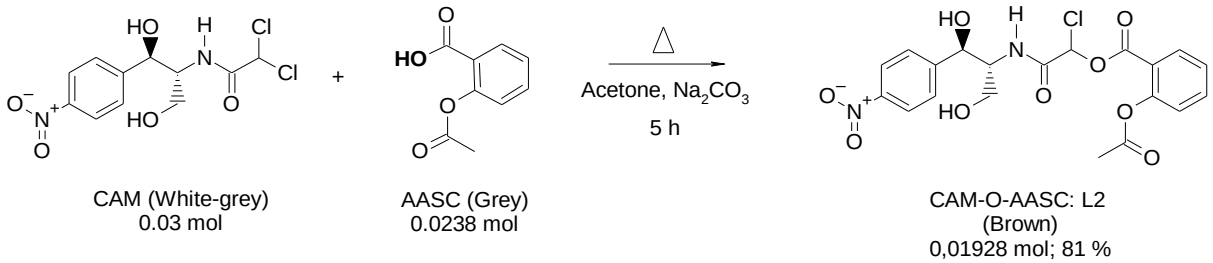

Figure 2: CAM-O-AASC synthesis equation

2.4.3. Synthesis of C1 complex "Iron- CAM-O-APP": 10 ml of an aqueous solution of hydrated iron chloride FeCl3.6H2O (0.0082 mole) and 10 ml of an ethanolic solution of CAM-O-APP (0.0164 mol) were mixed and heated under reflux with constant stirring for 3 hours. The reaction mixture was cooled and left for 48 hours for crystallization. The residue was filtered under reduced pressure and the crystals are washed with ethanol (Yield: 85.2%).

2.4.4. Synthesis of the C2 complex "Iron- CAM-O-ASC: 10 ml of an aqueous solution of hydrated iron chloride FeCl3.6H2O (0.0062 mol) and 10 ml of an ethanolic solution of CAM-O-ASC (0.0124 mol) were mixed and heated under reflux with constant stirring for 3 hours. The reaction mixture was cooled and left for 48 hours for crystallization. The residue was filtered under reduced pressure and the crystals are washed with ethanol (Yield: 76%).

2.4.5. Synthesis of C3 "Iron- CAM" complex: 10 ml of an aqueous solution of hydrated iron chloride FeCl3.6H2O (0.011 mol) and 10 ml of an ethanolic solution of CAM (0.022 mol) were mixed and heated under reflux with constant stirring for 3 hours. The reaction mixture was cooled and left for 48 hours for crystallization. The residue

was filtered and the yellow crystals were washed with ethanol (Yield: 70.5%). Finally, the purity was evaluated by TLC.

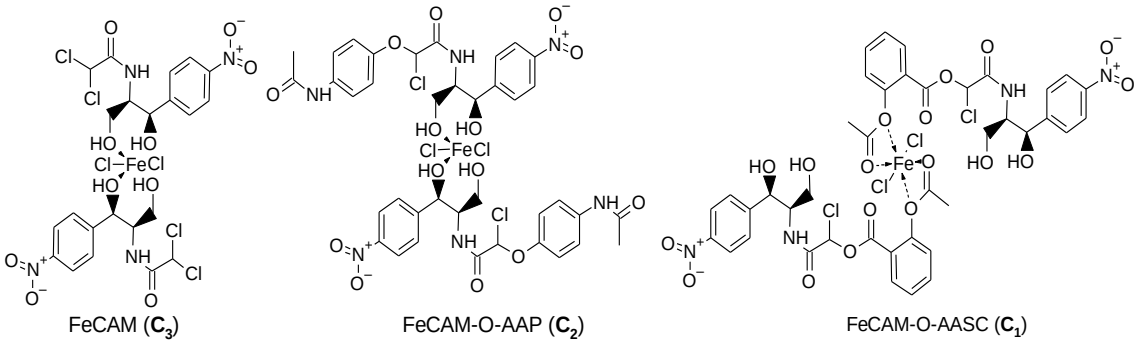

Figure 3: Probable structures of the complexes

2.4.6. Characterization by TLC: Weigh 0.02 g of the products studied (CAM-O-AAP or CAM-O-AASC), dissolve them in 2 ml of concentrated hydrochloric acid, and determine the presence of the starting substrate (CAM) in the mixture by TLC on a silicagel plate eluted by a mixture of methanol/ethyl acetate (5:5) and revealed by iodine.

3. Results and Discussion

3.1. Purification and identification of reagents

The substrate (CAM) and reagents were purified to separate them from the excipients. The pharmaceuticals were treated with several solvents to remove compounds such as starch, cellulose, talc, and others. The active substances were obtained in the form of white crystals with yields varying between 70 and 80% (CAM: 80%, AAP: 70%, and AASC: 79%). The identification tests of CAM, PAA, and AASC were positive. Indeed, the mixture of CAM, phenol and KOH, when boiled, produced a red-brown coloration. In addition, upon heating, in the presence of sodium hydroxide, a red-orange coloration was produced, and there was a release of ammonia. The identification of PAA was confirmed by the appearance of an intense blue coloration in the presence of ferric chloride [10]. The presence of AASC was confirmed by the release of acetic acid upon heating and obtaining a yellow color after intense heating. Furthermore, the addition of potassium hydroxide (in ethanol) in the presence of ferric chloride produced a purple color [10].

3.2. Synthesis and characterization of ligands and complexes

The ligands were synthesized from CAM as substrate with PAA for the synthesis of ligand L1 (Yellowish-white solid) on the one hand and with AASC for the synthesis of ligand L2 (Highly viscous brown liquid) on the other hand. All ligands were characterized by the presence of the R-O-R bond formed between the substrate and the reagent. All ligands were synthesized, purified and obtained with good yields, i.e. 91.12% for L1 and 81% for L2. Like the ligands, all the complexes were also synthesized, by reaction between the L1 ligands with iron to give the C1 complex (Greyish solid) and between the L2 ligand and iron to give the C2 complex (Red-brown solid) on the one hand as well as between CAM and iron giving the C3 complex (Yellow-red solid).

3.2.1. UV-Vis spectra: Generally, the ligands were also characterized by the presence of intra-ligand electronic transitions on their UV-Visible spectra in the wavelength range between 270 and 395 nm. The different synthesized products exhibited maximum absorbances at 335 for CAM, 325 for ligand L1, 395 for ligand L2, 330 nm for complex C1, 325 nm for complex C2 and 335 nm for complex C3.

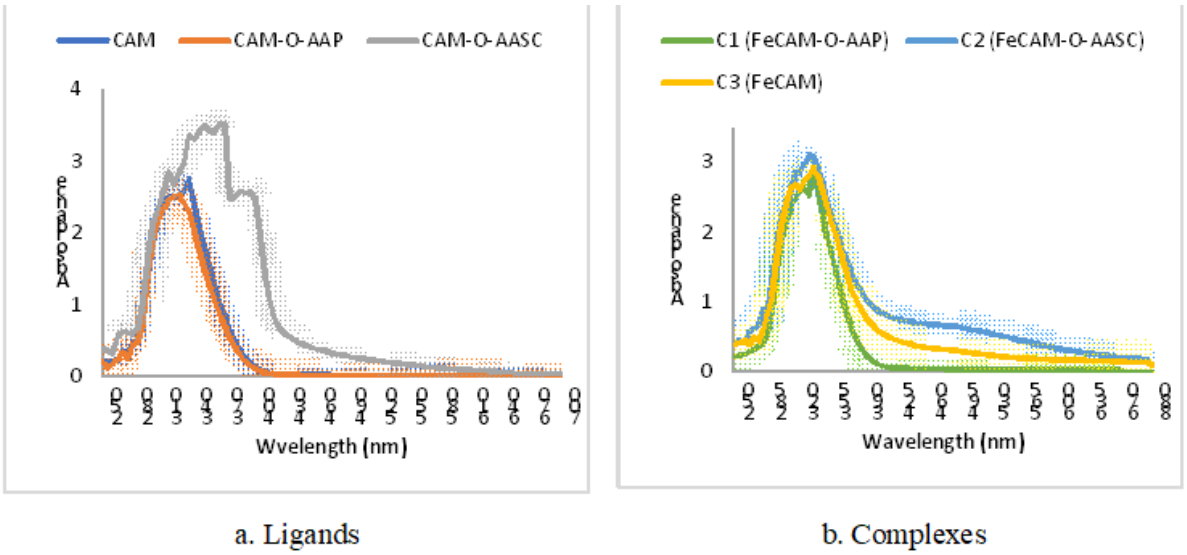

a. Ligands b. Complexes

Figure 4: UV-Vis spectra

The ligands showed bands and shoulders that were observed in the UV range. Some of them showed π → π* transitions (at 270 and 310 nm for CAM; at 270 and 280 nm for L1; at 315 and 370 nm for L2) that could be consistent with the C = C double bond, and others can be attributed to n → π* transitions (at 335 nm for CAM, at 325 nm for L1, and 395 nm for L2) that could well be consistent with the O-H, N-H, and C = O bonds. Moreover, the complexes show bands and shoulders corresponding to the characteristic electronic transitions of the ligands. In particular, it is the π → π* transitions (at 275 and 320 nm for C1; at 280 and 315 nm for C2; at 260 and 270 nm for C3) that would correspond to the C = C double bond and n → π* (at 325 nm for C1, 330 nm for C2 and 315 nm for C3) that would correspond to the O-H, N-H and C=O bonds. On the other hand, the complexes each show a shoulder at 335 nm corresponding to an MLCT (Metal to Ligand Charge Transfer) or d → π* transition between the iron and the ligand, characteristic to the complex formation.

By comparing the spectra of the L1 and L2 ligands with that of CAM, different effects were observed. These include the hypsochrome effect in the case of the L1 ligand (from 335 nm for CAM to 325 nm for L1) and the bathochrome effect that would be due to an extension of delocalization in the L2 ligand (from 335 nm for CAM to 395 nm for L2). These observations would thus be evidence for the formation of L1 and L2 compounds. In addition, the UV-Vis spectra of the C1, C2, and C3 complexes compared to the spectra of their respective ligands (L1, L2, and CAM) showed different types of effects, in particular the hyperchromatic effect in the case of the C1 and C3 complexes justified by the increase of the absorption maximum and the hypsochromatic effect in the case of C2 (from 395 nm for L2 to 315 nm for C2). These observations could well indicate the formation of C1, C2, and C3 complexes.

3.2.2. Computational modeling: The structure of CAM complexes and these derivatives are such that the ligands chelated the metal cation in a bidentate manner, and the coordination sphere was completed with halides (the chloride ions in this study) [14]. Thus, based on the experimental data, theoretical calculations were performed using the molecular mechanics method with UFF as the force field to determine the structures of the complexes. Based on the different energy values of the various hypothetical structures, it was found that only three structures (Figure 3) presented good stability and thus low electronic energy, namely 6844.26 kJ/mol for C1, 4467.63 kJ/mol for C2 and 6579.62 kJ/mol for C3 compared to the other proposed structures.

3.3. *In silico* prediction

3.3.1. Evaluation of five Lipinski's rule: The rule of five is used to determine the degree of absorption or permeability of compounds against lipid bilayers in the human body. It is a parameter that demonstrates the oral biological availability of a compound (Table 2). The pharmocokinetic parameters are estimated based on Lipinski's "rule of 5," in which a compound meets the drug-like criterion if:

- the molecular weight is less than 500 g/mol,
- the calculated octanol/water partition coefficient is less than 5 (Logp 5),
- the number of hydrogen bond donors (Nh And Oh Groups) is slightly less than 5,
- the number of hydrogen bond acceptors (especially N and O atoms) is less than 10.

Properties	Molar mass (g/mol)	**Log *P***	#Rotating bonds	#Hydrogen bond acceptors	#Hydrogen bond donors
CAM	323.132	0.909	6	5	3
L1	437.836	1.7076	9	7	4
L2	466.83	1.4525	9	9	3
C1	1060.411	4.9837	18	14	6
C2	1002.423	4.7917	14	10	4
C3	738.57	2.6296	8	6	2

Table 2: Molecular parameters of compounds according to PkCSM

Based on molecular properties (Table 2), it was found that CAM, L1, and L2 conformed to Lipinski's rule. Thus, these compounds would have good oral bioavailability. On the other hand, not all complexes complied with the rule of 5; however, complex C3 only violated the molecular mass criterion.

3.3.2. ADME prediction: The latter consists of the prediction of ADME properties. These were predicted using the PreADMET, and PkCSM tools (Table 3).

Parameters	**CAM**	**L1**	**L2**	**C1**	**C2**	**C3**
BBB	0.0334	0.0285	0.03851	0.0525	0.0389	0.0934
Caco2	17.5665	13.3206	15.5571	19.6709	19.1368	20.4127

CYP_2C19_inhibition	No	No	No	No	No	No
CYP_2C9_inhibition	No	Inhibitor	No	Inhibitor	Inhibitor	Inhibitor
CYP_2D6_inhibition	No	No	No	No	No	No
CYP_2D6_substrate	No	No	No	Weak	No	Weak
CYP_3A4_inhibition	Inhibitor	Inhibitor	Inhibitor	Inhibitor	Inhibitor	Inhibitor
CYP_3A4_substrate	Non	Weak	Substrat	Substrat	Substrat	Substrat
HIA	83.2759	76.06145	69.4471	92.8849	76.38	96.1361
MDCK	1.3436	0.3553	0.1801	0.018	0.018	0.0182
Pgp_inhibition	No	No	Inhibitor	Inhibitor	Inhibitor	Inhibitor
Plasma_Protein_Binding	65.9271	84.1694	89.0885	63.4831	52.7252	61.8173
Pure_water_solubility_mg_L	537.193	40.2848	25.85	7.34E-06	0.0139	0.0038
Skin_Permeability	-4.0534	-3.6491	-3.3071	-5.0403	-5.0796	-5.0082
P-glycoprotein substrate	Yes	Yes	Yes	Yes	Yes	Yes
VDss (humain : log L/kg)	-0.16	-0.008	-0.578	-0.719	-0.691	-0.879
Fraction unbound (humain)	0.35	0.055	0	0.107	0.163	0
CNS permeability	-3.113	-3.323	-3.661	-3.498	-4.089	-2.955
Total Clearance	0.281	-0.071	0.017	-0.827	-0.487	-0.473
Renal substrate OCT2	No	No	No	No	No	No

Table 3: ADME prediction according to PreADMET, and PkCSM

All the synthesized compounds (Table 3) have positive BBB penetration values with a better result for C3 (BBB: 0.0934), suggesting that they can all moderately cross the blood-brain barrier. However, these values are less than 1, this implies that they are inactive in the central nervous system. They showed positive values of PCC permeability, which could justify their moderate Caco-2 cell permeability, and again the best result was obtained with C3. They would all be inhibitors of CYP3A4 but only L2, C1, C2, and C3 are substrates while L1 is a weak substrate for CYP3A4, and they would be inhibitors of CYP2C9 except for L1 and L2. They are neither substrates of CYP2D6 nor inhibitors of CYP2C19. All compounds exhibited high human intestinal absorption (HIA) values in the range of 69 - 96%, the range of compounds that are well absorbed and thus can be assimilated through the human intestine (Rashid, 2020). All ligands exhibited low MDCK values except for CAM, which had the highest value, and thus exhibited high efficiency of absorption and penetration of the human intestinal barrier (Rashid, 2020). Except for CAM and L1, all compounds appeared to be effective in inhibiting P-glycoprotein (P-gp: main barrier for drug delivery and expulsion). Only the L2 presented an affinity for the plasma protein with an approximately high value of 89% (close to 90%), on the other hand, the other compounds would present a low affinity, and this influences the drug delivery process which is better in the case of L2. All the compounds under examination presented negative values of skin permeability, suggesting that it would not be important for the compounds to be administered by the transdermal route. Most drugs in plasma would exist in equilibrium between either an unbound or protein-bound state in serum. The effectiveness of a given drug may be affected by the degree to which it binds to proteins in the blood. Indeed, the more bound that molecule is, the lower the efficiency to cross the cell membrane and diffuse [15].

All ligands under examination showed a low value of the unbound fraction of which CAM possessed a better efficiency to cross the cell membrane and diffuse. CNS permeability is the measure of the penetration of a molecule or compound into the central nervous system. A compound, with a CNS permeability value greater than -2, is considered capable of penetrating the central nervous system, on the other hand, the one with a lower value, is considered incapable of penetrating the central nervous system. All the compounds under examination have values lower than -2, so they cannot penetrate the central nervous system. Organic cation transporter 2 (OCT2) is a renal uptake transporter that plays an important role in renal disposition and clearance of drugs and endogenous compounds. OCT2 substrates also have the potential for adverse interactions with coadministered OCT2 inhibitors. Assessment of a compound's potential to be transported by OCT2 provides useful information regarding not only its clearance but also potential contraindications. Drug clearance appears to be the combination of hepatic clearance (metabolism in the liver and biliary clearance) and renal clearance (excretion via the kidneys). All compounds were not likely substrates for OCT2, and showed negative values of total clearance except for CAM and L1, which have positive values and thus possess good extrusion.

3.3.3 Toxicity prediction: Similar to the prediction of ADME properties, the toxicity prediction was performed using the PreADMT and PkCSM tools (Table 4).

Parameters/Toxicity	CAM	L1	L2	C1	C2	C3
Algae_at	0.0673	0.0289	0.0223	6.87E-05	0.00037	0.00196
Ames_test	Mutagenic	Mutagenic	Mutagenic	Mutagenic	Mutagenic	Mutagenic
Carcino_Souris	Negative	Negative	Negative	-	-	-
Carcino_Rat	Negative	Negative	Negative	-	-	-
Daphnia_at	0.3996	0.182	0.1188	0.0011	0.0049	0.016
Inhibition_hERG	Low risk	High risk	Ambigu	Medium risk	Medium risk	Medium risk
TA100_10RLI	Negative	Negative	Negative	Negative	Negative	Negative
TA100_NA	Negative	Negative	Negative	Negative	Negative	Negative
TA1535_10RLI	Negative	Negative	Negative	Negative	Negative	Negative
Max. tolerated dose (log mg/kg/day)	0.717	-0.076	0.368	0.185	0.486	-0.753
Acute Oral Toxicity of Rat (LD_{50} : mol/kg)	2.437	2.606	2.234	2.367	2.487	1.964
Chronic Oral Toxicity of Rat (LOAEL : log mg/kg_bw/day)	2.022	2.34	2.363	4.33	4.215	3.112
Hepatotoxicity	No	Yes	Yes	Yes	Yes	No
Skin Sensitization	No	No	No	No	No	No
T. Pyriformis toxicity (log µg/L)	0.484	0.313	0.292	0.285	0.285	0.289
Toxicity of minnow (log mM)	1.727	2.6	2.297	-0.324	0.231	-1.466

Both tools revealed in general that the products studied are all mutagenic. However, for their hERG inhibition, CAM presented a low risk, L1 presented a high risk, and an equivocal result is obtained for L2. On the other hand, all

complexes (C1, C2, and C3) showed a medium risk. All studied compounds were negative in TA100_10RLI, TA100_NA and TA1535_10RLI toxicity tests and appeared to be hepatotoxic except for CAM and its C3 complex; they are not likely to be associated with skin sensitization. *Tetrahymena pyriformis* is a protozoan bacterium whose toxicity is often used as the limit or endpoint of toxicity. For a given compound, if the $plGC_{50}$ value (the negative logarithm of the concentration required for 50% growth inhibition) is greater than -0.5 log µg/L, that compound would be toxic [15]. All of the compounds tested, given that they have positive $plGC_{50}$ values and greater than -0.5 log µg/L, exhibited *T. Pyriformis*. In addition, minnow toxicity is expressed by the lethal concentration (LC50) values, which represent the concentration of a molecule required to cause the death of 50% of minnows. A compound is considered to have high acute toxicity if it has an LC_{50} value less than -0.3 [15]. All of the compounds tested had valued above -0.3, so they are non-toxic to minnow toxicity, except for C3, which had a value of -0.324.

3.3.4. Bioactivity scores: Prediction of the bioactivity score was performed using the Molinspiration tool (Table 5). Bioactivity is considered considerable when the bioactivity score is greater than 0.00; moderate when the bioactivity score is between -0.5 and 0.00 and inactive when the bioactivity score is less than -0.5 [16].

Compounds	**GPCR Ligand**	Ion channel modulation	Kinase inhibitor	ligand Nuclear receptor	Protease inhibitor	Enzyme inhibitor
CAM	-0.22	-0.28	-0.38	-0.41	-0.21	0
L1	-0.04	-0.17	-0.26	-0.18	-0.1	-0.09
L2	-0.08	-0.15	-0.37	-0.07	-0.11	-0.07
C1	-3.07	-3.59	-3.53	-3.56	-2.44	-3.39
C2	-3.51	-3.69	-3.68	-3.68	-3.15	-3.6
C3	-0.31	-0.63	-0.29	-0.42	-0.1	-0.31

Table 5: Bioactivity scores according to Molinspiration software

In general, all tested compounds showed good bioactivity with the best results obtained in the case of enzymatic inhibition with a better score attributed to CAM as the best enzymatic inhibitor compared to the other tested compounds. However, compounds L1 and L2 showed a better affinity for the GPCR ligand compared to CAM. Compounds L1, and L2 (Table 5) exhibited good ion channel modulation property with a high score assigned to compound L2 (-0.17). Compounds L1 and L2 also presented a better score as a Protease inhibitor compared to CAM (-0.10 for L1, and -0.11 for L2). However, compound L1 presented as a better kinase inhibitor compared to the other compounds. Compound L2 showed a high affinity for the nuclear receptor ligand followed by compound L1 and CAM. Regarding the complexes, they presented lower bioactivity than the ligands (CAM, L1 and L2). The best results were obtained in the case of Protease inhibition and Kinase inhibition with better scores attributed to the C3 complex. The latter appeared to be the compound with good bioactivity compared to the other complexes, besides its inhibitory activity on Kinase and Proteases, it presented a better affinity for the GPCR ligand and the nuclear receptor ligand, as well as a good modulation of the ion channel [17,18].

4. Conclusion

In this work, two derivatives of chloramphenicol and their iron complexes were synthesized to see the possibilities of improving the efficacy and pharmaceutical properties of chloramphenicol on the one hand and reducing its toxicity, consequently its side effects, on the other hand. The synthesized compounds were collected with a good yield and characterized by analytical (chemical), spectral and theoretical methods for the determination of the probable structures of the complexes. And these structures allowed a theoretical study (in silico prediction) of the biopharmaceutical properties of the compounds. In general, CAM, L1, and L2 show good similarities with drugs, good bioavailability and bioactivity since they were by Lipinski's five rule. The complexes, on the other hand, did not comply with Lipinski's rule. On the other hand, the ADME properties showed that C3 was presented a good efficiency of absorption and distribution in the organism about the other synthesized compounds and CAM as a reference compound. Concerning toxicity, all the compounds seemed to have toxicity almost identical to that of CAM. All the compounds studied have overall moderate bioactivity while L1 and L2 showed better bioactivity scores than the complexes. CAM showed only efficacy in enzyme inhibition. However, L1 and L2 ligands have better performance especially in kinase (score of -0.26 and -0.37 respectively for L1 and L2), protease (score of -0.10 for L1, and -0.11 for L2) inhibition. This suggests the ligands have better therapeutic performance and could well address several clinical needs. The synthesized compounds (L1 and L2) appeared to be potential candidates to substitute chloramphenicol, hence it could be interesting to continue the studies by preparing and characterizing (by advanced spectral methods) other derivatives, by adding other pharmacophoric moieties on chloramphenicol, and synthesizing their complexes; and finally to evaluate their biopharmaceutical properties by in silico predictions and by in vitro and in vivo studies on mice.

Credit authorship contribution statement

KME designed the study, KMM, LKE & KKO carried out the study, the analysis, the writing of the manuscript, the editing, the revision, the methodology with the help of MKM.

Declaration of competing ınterest

The authors declare that they have no potential competing interests

References

1. Neu HC, Fu KP. In vitro activity of chloramphenicol and thiamphenicol analogs. Antimicrobial agents and chemotherapy 18 (1980): 311-316.
2. Giannopoulou PC, Missiri DA, Kournoutou GG, et al. New Chloramphenicol Derivatives from the Viewpoint of Anticancer and Antimicrobial Activity. Antibiotics 8 (2019): 9.
3. Magoulasa GE, Kostopouloub ON, Garnelisa T, et al. Synthesis and antimicrobial activity of chloramphenicol polyamine conjugates. Bioorganic & Medicinal Chemistry 23 (2015): 3163-3174.
4. Dinos GP, Athanassopoulos CM, Missiri DA, et al. Chloramphenicol Derivatives as Antibacterial and Anticancer Agents: Historic Problems and Current Solutions. Antibiotics 5 (2016): 1-21.
5. Bartlett JG. Chloramphenicol. Symposium on Antimicrobila Therapy (1982).

6. Mullen GB, Georgi, VS. Adamantylmethyl Analogues of Chloramphenicol. Journal of Pharmaceutical Sciences 77 (1988): 7.
7. Bouchareb LF. Contribution à l'étude de la stabilité des complexes de « metaux-pyrazoles » par modélisation moléculaire. (Mémoire de magister), Université Abou-Bakar Belkaid De Tlemcen, Algérie (2016).
8. Ghannay S, Kadri A, Aouadi K. Synthesis, in vitro antimicrobial assessment, and computational investigation of pharmacokinetic and bioactivity properties of novel trifluoromethylated compounds using in silico ADME and toxicity prediction tools. Monatshefte für Chemie (2020).
9. Al-badr AA, El-Obeid, Humeida A. Chloramphenicol. American Pharmaceutical Association 15 (1986): 701-760.
10. European Pharmacopoeia (2020).
11. Omar MA, Amer HH, Nayelc M, et al. Synthesis and antimicrobial activity of new synthesized paracetamol derivatives and their acyclic nucleoside analogues. International Journal of Scientific and Research Publications 6 (2016): 4.
12. Lawal A, Obaleye JA. Synthesis, characterization and antibacterial activity of aspirin and paracetamol metal complexes. Nigerian Society for Experimental Biology 19 (2007): 9-15.
13. Sakuth M, Mensing T, Schuler J, et al. Ethers, Aliphatic. Wiley-VCH Verlag GmbH & Co. KGaA, Weinheim (2010).
14. Al-Khodir FA, Refat, Moamen S. Synthesis, spectroscopic, thermal and anticancer studies of metalantibiotic chelations: Ca(II), Fe(III), Pd(II) and Au(III) chloramphenicol complexes. Journal of Molecular Structure 1119 (2016): 157-166.
15. Pires DE, Blundell TL, Ascher DB. pkCSM: predicting small-molecule pharmacokinetic properties using. J Med Chem 58 (2015): 4066-4072.
16. Rashid M. Design, synthesis and ADMET prediction of bis-benzimidazole as anticancer agent. Bioorganic Chemistry 96 (2020): 2045-2068.
17. Daina A, Michielin O, Zoete V. SwissADME: a free web tool to evaluate pharmacokinetics, druglikeness and medicinal chemistry friendliness of small molecules. Scientific Reports 7 (2017): 42717.
18. Feng Z, Cao J, Zhang Q, et al. The drug likeness analysis of anti-inflammatory clerodane diterpenoids. Chinese Medicine 15 (2020): 126.